Advantages of T2SL – Results from production and new development at IRnova

Linda Höglund, C. Asplund, R. Marcks von Würtemberg, A. Gamfeldt, H. Kataria, D. Lantz, S. Smuk, E. Costard and H. Martijn

IRnova AB, Isafjordsgatan 22 C5, SE-16440 Kista, Sweden

ABSTRACT

IRnova has been manufacturing mid wave infrared (MWIR) detectors based on InAs/GaSb type-II superlattices (T2SL) since 2014. Results from the first years of production of MWIR focal plane arrays (FPAs) with 320 × 256 pixels on 30 μm pitch using the ISC9705 readout integrated circuit (ROIC) is presented in terms of operability, temporal and spatial noise equivalent temperature difference (NETD) and other key production parameters. Results on image stability of T2SL detectors show that no deterioration of image quality over time can be observed. Furthermore it is shown that the non-uniformity correction remains stable even after repeated detector temperature cycles. Spatial and temporal NETD for fabricated mid wave arrays show a temporal NETD of 12 mK and a spatial NETD of 4 mK with f/2 optics and 8 ms integration time. When studied over a large scene temperature, the spatial noise is still less than 60 % of the temporal noise. Furthermore, 640 × 512 mid wave FPAs with 15 μm pitch using the ISC0403 ROIC are entering an industrialization phase. Temporal and spatial NETD values of 25 mK and 10 mK, respectively, are obtained with f/4 optics and 22 ms integration time and the operability is 99.85 %. A status update on the development of T2SL detectors for short wave, mid wave and long wave infrared wavelength regions for existing and new applications is given and recent development towards higher operating temperature, smaller pitch and larger FPA formats is presented.

Keywords: heterostructure, infrared, detector, superlattice, InAs/GaSb

1. INTRODUCTION

In recent years InAs/InGaAsSb Type-II superlattices (T2SLs) have proven to be excellent material for high end infrared (IR) detectors and are now competing with the traditional state-of-the-art technologies. The desirable properties needed for good detector performance such as low dark current, high quantum efficiency (QE) and good focal plane array (FPA) performance have improved significantly in the last decade [1]. Initially, results on InAs/Ga(In)Sb superlattice (SL) detectors were mainly presented by research groups, but now both mid wave infrared (MWIR, 3-5 μm) and long wave infrared (LWIR, 8-12 μm) detectors based on T2SLs are mature enough to be manufactured by several companies [2]. One of the main reasons for the rapid improvement in detector performance is the novel barrier designs that utilize wide bandgap barriers to block the flow of majority carriers while allowing unimpeded transport of the minority carriers [3,4,5]. As a result of these barrier designs, strong reduction of the generation-recombination (G-R) dark current has been demonstrated, which results in improved detector performance [6,7,8].

T2SLs offer a great flexibility, as the bandgap (cut-off wavelength) of T2SLs can be tailored to any desired detection wavelength in the IR wavelength region by individually varying the thickness and composition of the alternating layers in the SL. In the past, different SL designs of the absorber have been utilized, using combinations of layers from the 6.1 Å material system (InAs, GaSb, AlSb) as well as alloys of these materials with InSb, AlAs and GaAs [8,9,10,11].

In this paper, results from InAs/GaSb T2SL detectors with cut-off wavelengths ranging from 2.4 μm to 12 μm are shown. With minor changes in the SL design, the cut-off wavelength can also be extended up to 16 μm which will be part of our future development. Statistics from the production of MWIR volatile organic compound (VOC) detectors is presented with the majority of the arrays having operabilities in the 99.8 – 99.9 % - range and with temporal and spatial noise equivalent temperature differences (NETDs) of 12 mK and 4 mK, respectively (the spatial NETD is a measure of the local non-uniformity across the array). Furthermore, excellent image correctability and image stability is demonstrated.

2. EXPERIMENTAL DETAILS

2.1 Material

Three structures with different cut-off wavelengths are presented in this paper, one MWIR structure (5.1 µm cut-off wavelength at 85K), one LWIR structure (12 µm cut-off wavelength at 80K) and one short wave infrared (SWIR) structure (2.7 µm cut-off wavelength at 300K). The MWIR structure (schematically illustrated in Figure 1) is a slightly modified and improved version of the epitaxial design reported in [12], and has been described in full detail in [13]. Similar designs as shown in Figure 1 were used for the LWIR and the SWIR detectors, but with the InAs, GaSb and AlSb layer thicknesses of the SLs slightly modified to change the bandgaps to the desired wavelength regions.

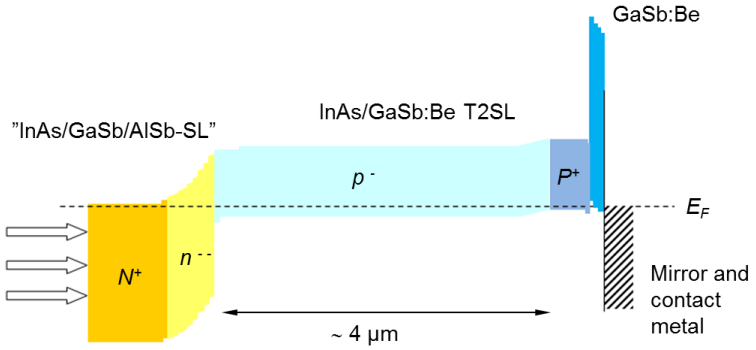

Figure 1. Double heterostructure (DH) detector design used in IRnova's detectors

2.2 Fabrication

To fabricate VOC detectors, 320 × 256 pixels detector arrays with 30 µm pixel pitch were produced from the MWIR structure using standard III/V processing techniques. Stepper lithography was used to define the pixels. Pixels were formed by a combination of dry and wet etching [14] and passivated using a dielectric passivation [15]. Mirror, contact metal and indium bumps were evaporated onto the pixels before dicing. The arrays were then hybridized to the read out integrated circuit (ROIC) ISC9705, underfill was deposited and finally the GaSb substrate was fully removed. The MWIR FPAs are using an anti-reflective (AR) coating optimized for detection at 3.3 µm. The FPAs were then mounted on a ceramic carrier, wire-bonded and put in a cooled test dewar with f/2 optics for tests of imaging performance. When applicable, a cold passband filter at 3.1-3.575 µm was used.

3. RESULTS

3.1 320 × 256 MWIR FPAs for gas detection of volatile organic compounds (VOC)

Gas detection is an emerging industrial application for high end infrared detectors. Many gases are transparent at most infrared wavelengths, but some gases have absorption in the infrared regions. In the MWIR range there is a large group of volatile organic compounds (methane, butane, propane etc.) that exhibit absorption (and radiation) peaks around 3.3 µm. By using a pass band filter, the detection is limited to the region of interest and the contrast is increased. This method can be used for visualization and documentation in real time of gas leaks.

VOC detectors fabricated from the MWIR T2SL material show good performance, both in terms of **QE and dark current.** In figure 2a, the external QE is shown for an FPA with light entering from the backside and AR coating

applied. The AR-coating was optimized to give minimum reflection at 3.3 µm and the resulting QE in the gas band (3-3.5 um) was ~50-55%. There is only a minor temperature dependence of the QE for wavelengths < 4.5 um. For wavelengths > 4.5 um, there is an increase of the QE with temperature, mainly due to shift of the cut-off wavelength (bandgap shift) with temperature. The dark current density at the operating bias (-0.1 V) was $\leq 1 \times 10^{-5}$ A/cm^2 for all temperatures ≤ 120 K (figure 2b), which allows for high temperature operation.

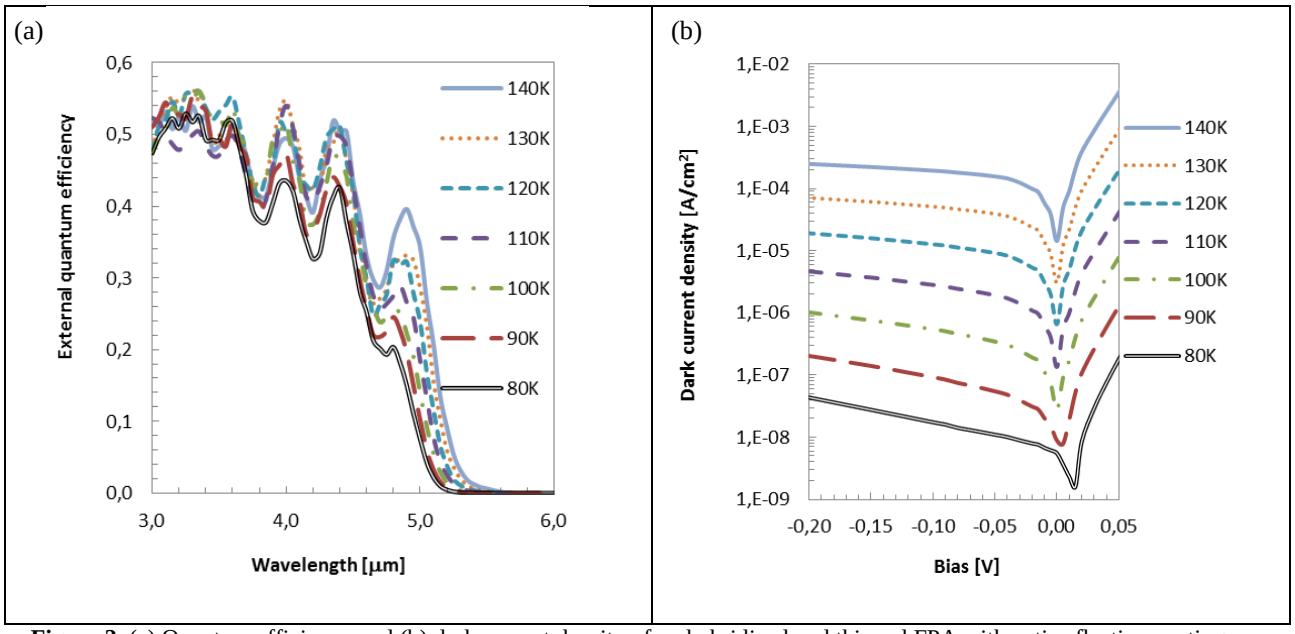

Figure 2. (a) Quantum efficiency and (b) dark current density of an hybridized and thinned FPA with anti-reflection coating optimized for 3.3 µm.

The **temporal and spatial noise** is studied routinely for all fabricated MWIR FPAs with the measurement conditions: F#2, T = 80-85 K, integration time about 8 ms. The **temporal noise** was obtained from a series of raw images taken with a 30 °C black body source giving a well fill of about 50%. First, the standard deviation of each pixel in time is calculated. Then, the NETD is calculated for each pixel, by dividing the median of these standard deviations with the response per Kelvin. Statistics from the fabricated FPAs (Figure 3a) shows that the average **temporal NETD** is on the order of **12 mK**, very close to the theoretical limit for a background limited detector. Furthermore, the temporal noise distributions for these FPAs are very narrow as demonstrated in Figure 3b. The **spatial noise** is a measure of how much pixels deviate statistically from their neighbors. To calculate the spatial NETD a series of non-uniformity corrected images are taken against a black body with a temperature half way between the two black body temperatures used for the non-uniformity correction (NUC) (30 °C and 40 °C in this case). The median value in time of each pixel is then calculated to generate a single image (minimizing the effect of temporal noise). This image is then divided into blocks of 5×5 pixels, and the standard deviation of all pixel values in each block is calculated. The spatial NETD is the median of all these standard deviation values divided by the response per Kelvin. Statistics from the fabricated FPAs (Figure 3a) shows that the average **spatial NETD** is approximately **4 mK**. When increasing the temperature above 85 K, both temporal and spatial NETD stays approximately the same for all temperatures < 100 K (Figure 3c). Minor increases of the NETD levels are observed in the temperature interval 100 – 110 K. For temperatures above 110 K, the spatial noise starts to increase more rapidly. Excellent temporal image stability is also observed, with no deterioration of the image quality (spatial noise) with time (Figure 3d). This gives proof to the excellent imaging properties of these detectors, with stability after NUC comparable to QWIP behavior.

Spatial and temporal noise levels have also been used to study the **image stability** of the MWIR detectors. In this study, the integration time was set to 1 ms in order to cover a wider temperature range. In the two-point NUC, the spatial noise was cancelled out at two temperatures (25 °C and 70 °C) using two different black body sources (see Figure 3e). 100% correctablility is obtained in the two NUC points and in the temperature range between the two NUC points, the spatial noise is < 60% of the temporal noise in the whole temperature range (Figure 3e). Even after several temperature cycles

of the array, only a minor increase of the spatial noise is observed. This stability and image correctability in such a large temperature span proves that both the detector material and the ROIC are very robust, with a linear behavior in a very large dynamic range.

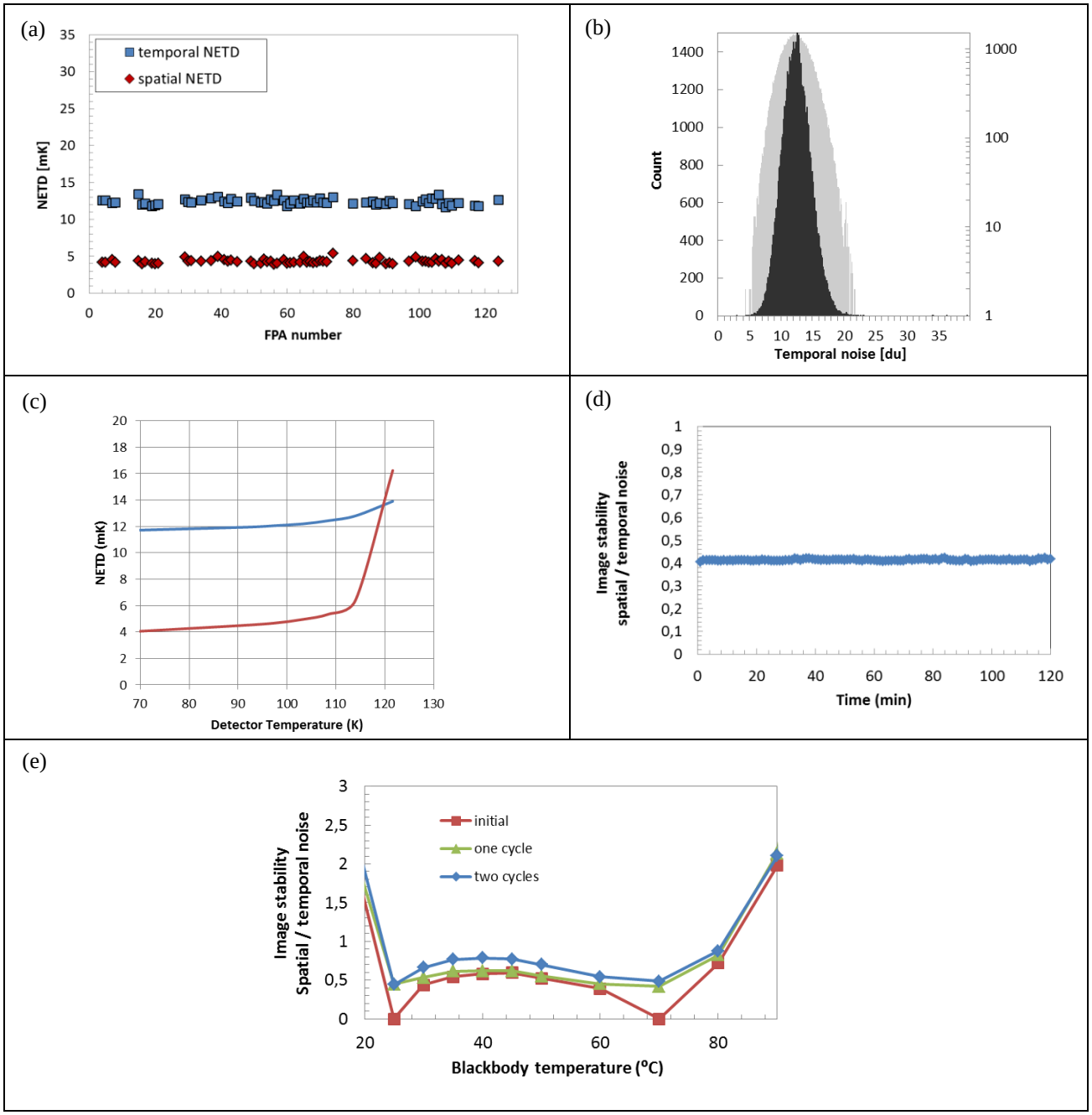

Figure 3. (a) Statistics of temporal and spatial NETD for a multitude of FPAs at 85 K, with NUC temperatures 30 °C and 40 °C and spatial noise measured at 35 °C. (b) Noise histogram of the temporal noise, with corresponding median temporal NETD of 12 mK, integration time 8 ms, F/2 optics and T = 85 K. (c) Temperature dependence of the temporal and the spatial NETD for an MWIR detector from 70 to 120 K. (d) Spatial noise versus time showing the image stability over time for an MWIR FPA (operating temperature = 85K) (e) Spatial noise versus black body temperature showing correctability and image stability after several temperature cycles for an FPA operated at 85 K (2-point correction were performed at 25 °C and 70 °C).

Statistics from the **operability** of the VOC FPAs is shown in Figure 4a. A pixel is defined as non-operable when its response is deviating more than 7.5 % from its neighbors, if the temporal NETD >120 mK or if the spatial NETD > 80 mK. The majority of the arrays have operabilities in the range 99.8 – 99.9 %. Statistics on cluster sizes of the non-operating pixels are presented in Figure 4b and these are divided into four regions on the FPA; A1-A4 where A1 represents the center and A4 the outer region. For the non-operating pixels most clusters have less than four pixels. Clusters larger than four pixels are very rare in the VOC FPA production and only appear in the outer region of the FPA (Figure 4b). This distribution is very desirable since the image quality is not affected as much by small clusters in the center area as by large clusters in that region.

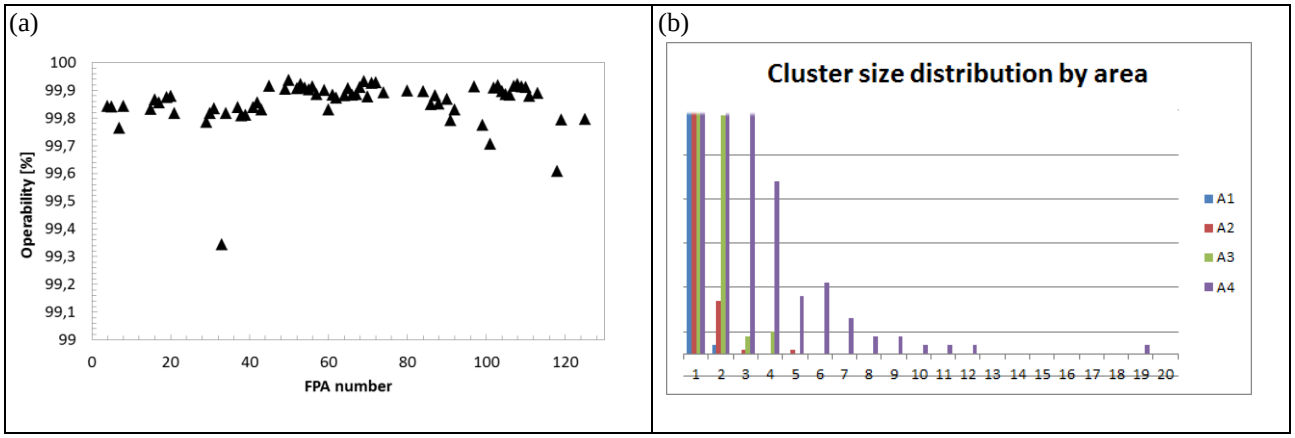

Figure 4. (a) Statistics of the operability for a multitude of VOC FPAs showing that most FPAs have operabilities in the range 99.8 – 99.9%. (b) Statistics of the cluster size distribution of non-operating pixels (full scale not shown) illustrating that most clusters have less than 4 pixels. The labeling A1 – A4 refers to the region on the FPA where A1 is the center region and A4 corresponds to the outer region. Larger clusters are rare in the fabricated VOC FPA production and only appear in the outer region of the FPA.

Exellent gas contrast is demonstrated for a VOC integrated dewar-cooler assembly (IDCA) with pass band filter mounted in the camera (Figure 5). The images are taken from a movie of two men filling up their car with natural gas (methane gas). When removing the nozzle, a methane cloud is seen around the nozzle (seen as a black cloud in figure 5).

Figure 5. Detection of methane gas with a VOC detector, taken with an IR camera with an IRnova 320 × 256 VOC FPA inside (mounted in an IDCA). When removing the nozzle, a methane cloud (seen as a black cloud in the images) is seen around the nozzle.

3.2 Development of 640 × 512 MWIR detectors

Work is in progress to also launch 640 × 512 MWIR FPAs with 15 µm pitch, utilizing the ISC0403 as read out circuit. The semiconductor process as well as the hybridisation process has been adjusted to these larger format arrays. The methodology described in section 3.1 was used to extract temporal and spatial NETD values, but with the measurement conditions: F#4, T = 85 K and integration time = 22 ms. The **temporal NETD** measure **25 mK** and the **spatial NETD is 10 mK.** The noise distribution is shown in Figure 6(a) and as expected for type-II superlattices, the noise level is low with a narrow temporal noise distribution. The average **operability** of these FPAs is 99.85 % (with the same definition of non-operating pixels as described in section 3.1). Both NETD results and operability is comparable to the 320 × 256 FPA statistics, when taking the different f-numbers into account. An IR-image taken with a 640 × 512 FPA mounted in a demonstrator under these conditions is shown in figure 6b.

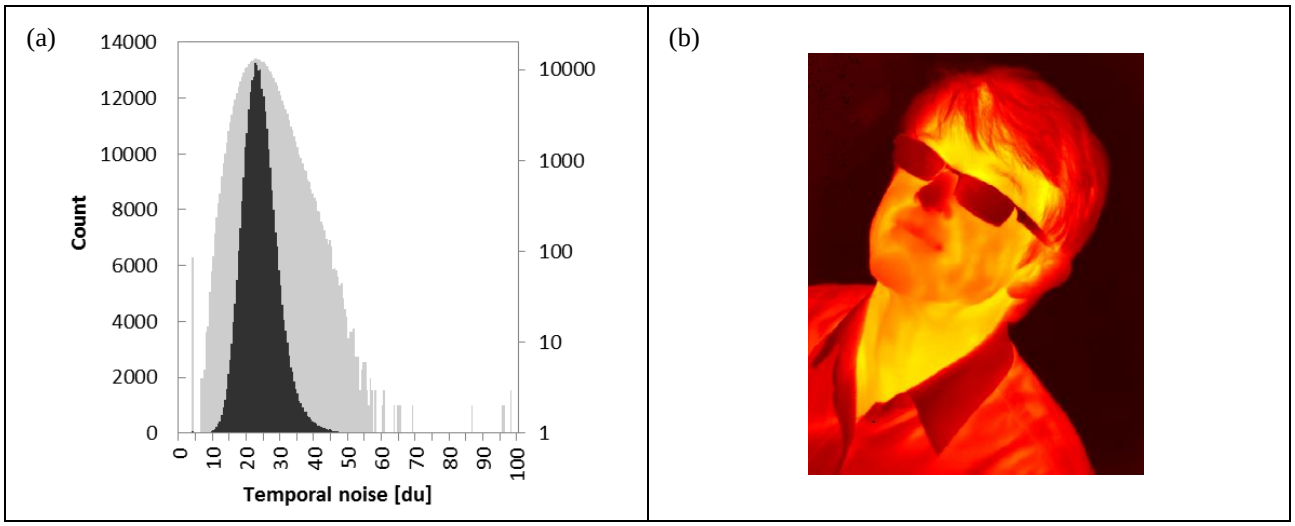

Figure 6. (a) Noise histogram, with a median temporal NETD of 25 mK, integration time 22 ms, F/4 optics and T = 85 K (b) IR image taken with 640 × 512 FPA utilizing the ISC0403 ROIC.

3.3 LWIR and VLWIR detectors for space applications

Large size 2D arrays for detection up to about 16 µm are mandatory for future space applications, particularly for weather forecast and atmospheric sounding missions. For these missions both high QE and low dark current is required. Mercury-Cadmium-Telluride (MCT) is currently the detector of choice for these applications, however the operability of MCT arrays in this wavelength region is low and the performance of operable pixels degrade with time. T2SL is recognized as the most promising alternative to MCT for 2D LWIR and very long wave infrared (VLWIR, ~12 - 30 µm) array production, and would presumably give better uniformity and operability. IRnova is currently developing detectors for these applications, starting with LWIR detectors with 12 µm cut-off wavelength. The initial results from single pixel detectors are very promising with dark current values only 3-4 times higher than Rule-07 for unpassivated devices (Fig. 7a) and with very low turn on bias of the detector response (Fig. 7b). The next step is to adapt the FPA processing, including passivation and AR-coating to these cut-off wavelengths and then to extend the cut-off wavelengths to 14.5 µm and 16.5 µm.

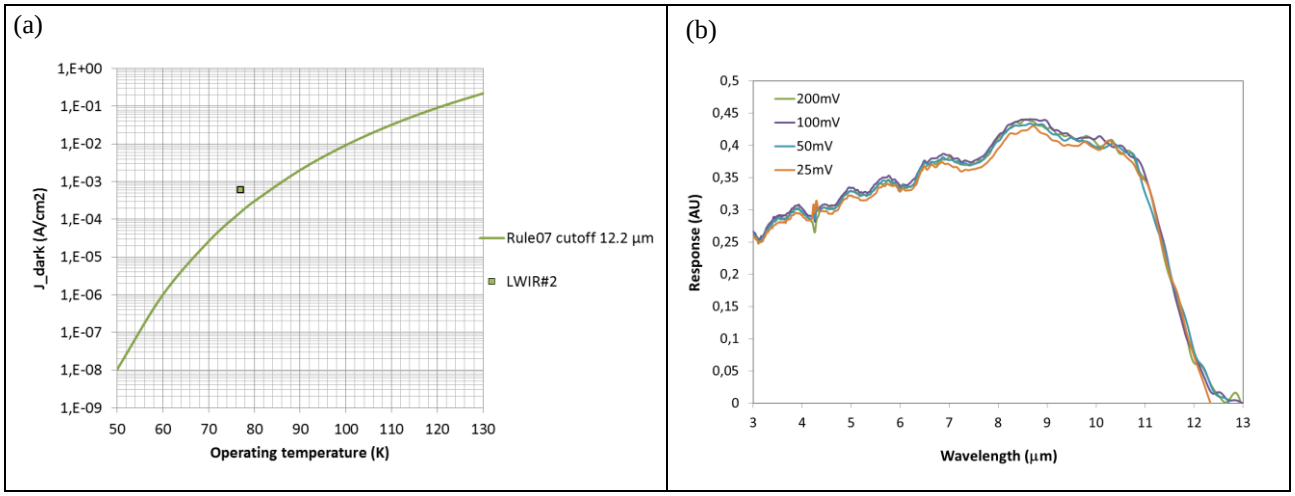

Figure 7. Dark current and response of a 12.2 µm LWIR detector operated at 77K (a) Comparison of T2SL dark current density with Rule-07 shows that the dark current density is only 3-4 times higher than Rule-07 (b) Response at different biases, showing that the response is fully turned on already at 25 mV.

3.4 SWIR detectors for space applications

The drive in earth observation towards better image quality and cost effective systems translates into mandatory improvements in detector technology. Detectors operating at higher temperatures allow for other more robust cooling technologies (for instance Stirling coolers vs thermo-electric coolers). Higher pixel count requires either smaller pixels or larger array sizes; both can only be realized with highly uniform detector materials. Uniformity and manufacturability of large detectors have been shown to be an Achilles heel of II/VI technology. T2SL on the other hand is a stable V/III material where the cut-off wavelength is defined by thicknesses of individual layers of InAs and GaSb. With molecular beam epitaxy (MBE) it is possible to grow high quality T2SL material with monolayer precision, which allows for good uniformity over large areas.

In the development of a SWIR detector at IRnova, a barrier, a contact layer and an absorber were designed for a DH detector structure as illustrated in Figure 1. The absorber cut-off wavelength at 77 K measured 2.4 µm and when the temperature was increased to 298 K, the cut-off wavelength shifted to 2.7 µm (Figure 8), which correlates well with the design of the absorber.

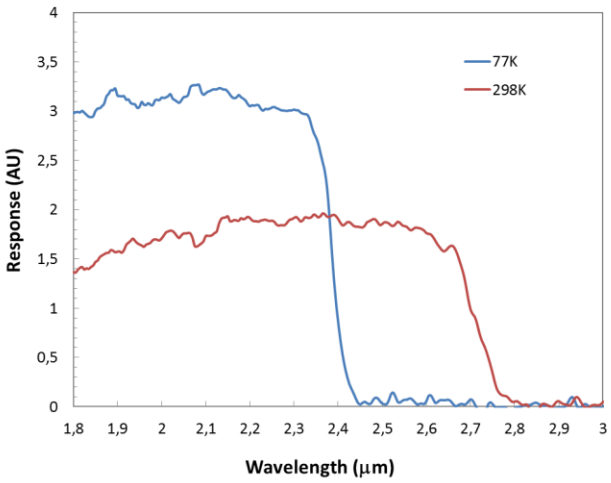

Figure 8. Spectral response of a SWIR detector. A shift in cut-off wavelength from 2.4 µm to 2.7 µm was observed when the temperature was increased from 77 K to 298 K, as anticipated from our modeling.

3.5 1280 × 1024 MWIR and LWIR FPAs for medical applications

IRnova is part of an EU-project (MINERVA), in which an instrument for infrared spectroscopy is developed. This will be used for improved medical diagnostics of cancer (http://minerva-project.eu/). Within the project, IRnova's task is to develop and manufacture a 1280 × 1024 pixel imaging detector, which will be part of the MINERVA demonstration instrument. This task is being carried out together with XeniCs, who provides IRnova with an ROIC and in a later stage will complement the IDCA manufactured at IRnova, with mechanical frame and case, optics and electronics to make it a camera.

IRnova has started the development of high resolution FPAs with cut-off wavelengths at 5.3 µm and at 12 µm, targeting operating temperatures of 120 K and 100 K, respectively. Similar superlattice designs as described in sections *3.1* and *3.2* have been used however, the semiconductor process as well as the hybridisation process for the larger format arrays have been developed within this project. The FPA resolution is 1280 × 1024 with 12 µm pitch. Test FPAs have been hybridized successfully (Figure 9a) and are awaiting full FPA characterization before integration in an IDCA (Figure 9b). Upon completion, such detectors would without doubt be state-of-the-art for the current commercial IR-technology.

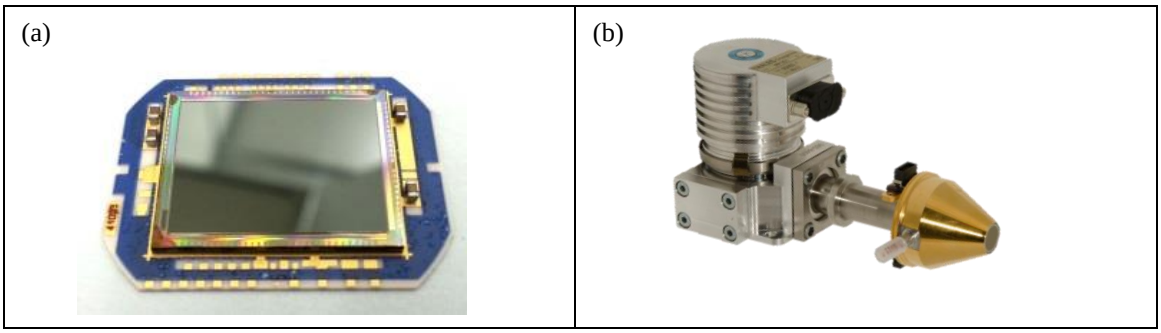

Figure 9. (a) Photo of newly hybridised FPA (b) Photo of the final IDCA.

First characterization results from the MWIR FPAs with 12 µm pitch are available. The peak QE, measuring 30% at 80 K (Figure 10) is fair and will be further improved by applying antireflective coating.

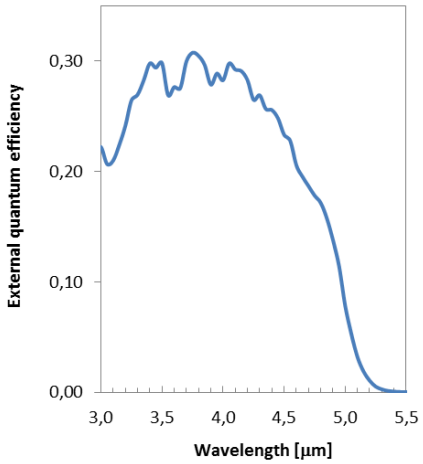

Figure 10. External quantum efficiency of the MWIR sample array without antireflective coating at 80K. The sample is a part of the fully processed detector chip hybridized to a specially designed fan-out chip. No ROIC was involved in the measurements.

4. SUMMARY

In this article, results from production and development of SWIR, MWIR and LWIR type-II superlattice InAs/GaSb detectors have been presented. Statistics from the production of high performance MWIR detectors were summarized, showing that high operability (99.8-99.9%) and low temporal and spatial NETD values (12 mK and 4 mK, respectively) are obtained routinely. The image stability was also demonstrated showing that the spatial noise remains low with several temperature cycles of the detector and that no deterioration of the image quality with time could be observed. Promising results were presented from the development of LWIR, SWIR and large format MWIR detectors.

5. ACKNOWLEDGEMENTS

We would like to thank the European Commission for sponsoring part of this work through the EU FP7 project MINERVA. We would also like to thank ESA for sponsoring work on SWIR and VLWIR superlattice detectors in the projects ITI-SWIR and Low Dark current VLWIR T2SL infrared detectors.

REFERENCES

[1] Ting, D., Soibel, A., Hoglund, L., Nguyen, J., Hill, C., Khoshakhlagh, A., Gunapala S.D. [Semiconductors and Semimetals], "Adv. Infrared Photodetect." 84 , 1–57 (2011).
[2] AIM (www.aim-ir.com), IRnova (www.ir-nova.se), SCD (www.scd.co.il), Qmagic (www.qmagic.com)
[3] White, A. M., "Infrared detectors", USA Patent 4,679,063 (1987)
[4] Maimon, S. and Wicks, G. W., " detector, an infrared detector with reduced dark current and higher operating temperature", Appl. Phys. Lett. 89, 151109 (2006)
[5] Klipstein, P., ""XBn " barrier photodetectors for high sensitivity and high operating temperature infrared sensors", Proc. of SPIE, 6940, 151109 (2009)

[6] Vurgaftman, I., Aifer, E., Canedy, C., Tischler, J., Meyer, J., Warner, J., Jackson, E., Hildebrandt, G., Sullivan, G., "Graded bandgap for dark current suppression in long-wave infrared W-structured type-II Superlattice photodiodes", Appl. Phys. Lett. 89 (12) 121114 (2006)
[7] Soibel, A., Rafol, S. B., Khoshakhlagh, A., Nguyen, J., Hoeglund, L., Keo, S. A., Mumolo, J. M., Liu, J., Liao, A., Ting, D. Z. Y., Gunapala, S. D., "Long wavelength infrared Superlattice detectors and FPAs based on CBIRD design", IEEE Photonics Technol. Lett. 25 (9) 875-878 (2013).
[8] Fuchs, F., Weimer, U., Pletschen, W., Schmitz, J., Ahlswere, E., Walter, M., Wagner, J., and Koidl, P., "High performance Superlattice infrared photodiodes", Appl. Phys. Lett. **71**(22), 3251-3253 (1997)
[9] Aifer, E. H., Tischler, J. G., Warner, J. H., Vurgaftman, I., Bewley, W. W., Meyer, J. R., Kim, J. C., Whitman, L. J., Canedy, C. L., and Jackson, E. M., "W-structured type-II long-wave infrared photodiodes with high quantum efficiency"Appl. Phys. Lett. **89**, 053519 (2006)
[10] Nguyen, B. –M., Hoffman, D., Delaunay, P. –Y. and Razeghi, M., "nBn detector, an infrared photodetector with reduced dark current and higher operating temperature",Appl. Phys. Lett. **91**(16) 163511 (2007)
[11] Ting, D. Z. –Y., Hill, C. J., Soibel, A., Keo, S., Mumolo, J.M., Nguyen, J., and Gunapala, S. D., "A high-performance long wavelength superlattice complementary barrier infrared photodetector "Appl. Phys. Lett. **95(**2), 023508 (2009)
[12] Asplund, C., Marcks von Würtemberg, R., Lantz, D., Malm, H., Martijn, H., Plis, E., Gautam, N. and Krishna, S., "Performance of mid-wave T2SL detectors with heterojunction barriers", Infrared Physics & Technology 59 (2013) 22–27.
[13] Malm, H., Gamfeldt, A., Marcks von Würtemberg, R., Lantz, D., Asplund, C., Martijn, H., "High image quality type-II Superlattice detector for 3.3 μm detection of volatile organic compounds", Infrared Physics & Technology 70, 34–39 (2015)
[14] Chaghi, R., Cervera, C., Aït-Kaci, H., Grech, P., Rodriguez, J. B. and Christol, P., "Wet etching and chemical polishing of InAs / GaSb superlattice photodiodes", Semicond. Sci. Technol. 24, 065010 (2009).
[15] Martijn, H., Asplund, C., Marcks von Würtemberg, R. and Malm, H.,"High performance MWIR type-II superlattice detectors", Infrared Technology and Applications XXXIX, Proc. of SPIE Vol. 8704, 87040Z (2013).